



ARTICLE

Asiatic acid alleviates ischemic myocardial injury in mice by modulating mitophagy- and glycophyagy-based energy metabolism

Fan Qiu^{1,2}, Yi Yuan¹, Wei Luo^{1,2}, Yan-shan Gong¹, Zhong-ming Zhang³, Zhong-min Liu^{1,2,4,5} and Ling Gao^{1,4,5}

Myocardial infarction (MI) causes disturbances in myocardial energy metabolism, ultimately leading to a poor prognosis. Cytosolic glycogen autophagy (glycophagy) and mitochondrial autophagy (mitophagy) are upregulated in MI to optimize energy metabolism but to a limited extent. Asiatic acid (AA), a pentacyclic triterpene derived from the traditional Chinese herb *Centella asiatica*, displays anti-inflammatory, antioxidant, and antiapoptotic activities. AA has been found to alleviate focal cerebral and liver ischemic injury by reversing mitochondrial dysfunction. In this study, we investigated whether AA exerted cardioprotective effects against MI by activating glycophagy and mitophagy to improve the energy balance. In vitro cardioprotective effects were examined in neonatal mouse cardiomyocytes subjected to oxygen-glucose deprivation for 12 h. Treatment with AA (2–50 μM) significantly increased cell viability and improved the energy metabolism evidenced by increased ATP level and phosphocreatine/ATP ratio. In vivo cardioprotective effects were studied in a mouse model of MI. Administration of AA (5–125 $\text{mg}\cdot\text{kg}^{-1}\cdot\text{d}^{-1}$, ig) significantly reduced infarct size and ischemic myocardial injury, and improved cardiac function. AA treatment also promoted mitophagy and relieved mitochondrial edema evidenced by increased number of mitophagosomes in ischemic myocardium in vivo and increased mitochondria-light chain 3 (LC3)-II colocalization in ODG-treated cardiomyocytes in vitro. Mitophagy activation was accompanied by activation of the AMPK signaling pathway. Knockdown of AMPK abolished AA-activated mitophagy. Furthermore, we showed that glycophagy was upregulated in OGD cardiomyocytes evidenced by increased starch binding domain protein 1 (STBD1)-GABA type A receptor-associated protein-like 1 (GABARAPL1) interaction and extracellular acidification rate, whereas AA treatment further promoted glycophagy accompanied by PI3K/Akt activation. PI3K inhibitor LY294002 or Akt inhibitor GSK690693 blocked the effects of AA on glycophagy and glycolysis. Finally, simultaneous inhibition of glycophagy and mitophagy abolished the cardioprotective effects and energy regulation of AA. These results demonstrate that AA protects ischemic cardiomyocytes by modulating glycophagy- and mitophagy-based energy metabolism through the PI3K/Akt and AMPK pathways.

Keywords: myocardial infarction; asiatic acid; glycophagy; mitophagy; energy metabolism; AMPK signaling

Acta Pharmacologica Sinica (2022) 43:1395–1407; <https://doi.org/10.1038/s41401-021-00763-9>

INTRODUCTION

Myocardial infarction (MI), the primary component of cardiovascular disease, is one of the leading causes of morbidity and mortality worldwide [1]. Despite treatment advances in recent years, the global medical burden caused by MI remains high [2]. Cardiac mitochondria are responsible for energy production and cardiomyocyte death; their integrity and dynamic nature, which are maintained by their intrinsic proteolytic system, are crucial for cell homeostasis [3]. Under ischemic conditions, ATP and creatine depletion due to mitochondrial injury result in functional and structural left ventricular alterations related to lower myocardial energy reserves [4]. Energy metabolism dysfunction leads to excess mortality from ventricular arrhythmias and progressive heart failure [4]. Therefore, agents that modulate energy homeostasis in MI may be promising therapeutic candidates.

Asiatic acid (AA) is a pentacyclic triterpene derived from *Centella asiatica*, which has anti-inflammatory, antioxidant, and antiapoptotic effects [5–8]. AA has long been used in herbal therapy for wounds and skin disorders [9]. It is detectable in human serum after oral administration [10], and it causes no significant toxicity in mice after either oral or subcutaneous administration [9]. AA exerts protective effects on focal cerebral ischemia and hepatic ischemia/reperfusion injury by ameliorating oxidative stress and maintaining mitochondrial homeostasis [7, 11], suggesting that it may be a potential therapeutic for mitochondrial and energy metabolism homeostasis.

Mitochondrial autophagy (mitophagy) is a specific autophagic process that selectively degrades damaged mitochondria to decrease reactive oxygen species release and protect against cell apoptosis [3]. Therefore, enhanced mitophagy is important for mitochondrial homeostasis and cardiomyocyte survival during ischemia, hypoxia,

¹Translational Medical Center for Stem Cell Therapy & Institute for Regenerative Medicine, Shanghai East Hospital, Tongji University School of Medicine, Shanghai 200123, China;

²Department of Cardiovascular and Thoracic Surgery, Shanghai East Hospital, Tongji University School of Medicine, Shanghai 200120, China; ³Department of Cardiovascular and Thoracic Surgery, Affiliated Hospital of Xuzhou Medical University, Xuzhou 221006, China; ⁴Shanghai Institute of Stem Cell Research and Clinical translation, Shanghai East Hospital, Tongji University, Shanghai 200120, China and ⁵Shanghai Engineering Research Center for Stem Cell Clinical Treatment, Shanghai 200123, China

Correspondence: Ling Gao (gaoleng5@126.com) or Zhong-min Liu (liu.zhongmin@tongji.edu.cn)

Received: 2 March 2021 Accepted: 10 August 2021

Published online: 14 September 2021

and/or other energy shortages [12]. Among the regulators of mitophagy, AMP-activated protein kinase (AMPK) is a classic activator that responds to cell energy stress; it works via various mechanisms, involving inhibition of the mammalian target of rapamycin complex and phosphorylation and activation of Unc-51-like kinase 1 (ULK1) [13]. Phosphorylation of a conserved threonine residue (Thr172) by upstream kinases is essential for AMPK activation [14]. In addition, light chain 3 (LC3) is also considered a modulator of mitophagy. LC3-I is lipidated to LC3-II to induce autophagosome formation, and LC3 lipidation results in an elevated LC3-II/LC3-I ratio or LC3-II expression, which is often used as a marker for mitophagy in numerous tissues, including myocardial tissue [15]. However, it is unclear whether AA maintains mitochondrial and energy homeostasis to protect the ischemic myocardium via mitophagic regulation.

In addition, glycogen autophagy (glycophagy) is a glycogen degradation and utilization process, which triggers liberation of free glucose that can be rapidly utilized by cells with energy requirements [16]. This process is a link between glucose homeostasis and autophagy in neonatal and adult cardiomyocytes, hepatocytes, and other organ cells under conditions of demand for glucose production [17]. Increased glycophagy provides a sufficient supply of glucose to ischemic cardiomyocytes for essential energy metabolism [18]. The potential mechanism of glycophagy involves the binding of starch binding domain protein 1 (STBD1) and the autophagy-related protein 8 (Atg8) family member, GABA type A receptor-associated protein-like 1 (GABARAPL1). STBD1, which consists of a carbohydrate-binding domain and an Atg8-interacting motif, is localized to the glycogen particle and plays an important role in intracellular glycogen trafficking to autophagosome by interacting with GABARAPL1, thereby constituting a specific mechanism of glycophagy [19, 20]. However, it remains unknown whether AA improves the energy supply after MI by regulating glycophagy.

The aims of this study were to determine the energy modulation and cardioprotective effects of AA on oxygen-glucose deprivation (OGD)-treated cardiomyocytes and a mouse MI model, investigate whether mitophagy and glycophagy are responsible for the energy metabolism and protective roles of AA, and elucidate the mechanisms underlying the effects of AA on mitophagy and glycophagy.

MATERIALS AND METHODS

Isolation and culture of neonatal mouse ventricular cardiomyocytes

Neonatal cardiomyocytes were isolated from one-day-old C57BL/6 mice [21]. Briefly, neonatal mice were anesthetized with sodium pentobarbital and sacrificed. Their hearts were removed and rapidly placed on ice. Then, the ventricles were dissected, minced into 1-mm³ pieces, transferred to a sterile tube, and washed in cold phosphate-buffered saline (PBS) to remove blood clots. Minced tissue was digested in PBS supplemented with 1 mg/mL trypsin, 1 mg/mL collagenase type II, and 0.2 mg/mL glucose for 5 min at 37 °C, and incubated with 0.1 mmol/L BrdU to selectively enrich for cardiomyocytes by inhibiting the growth of cardiac fibroblasts. Cardiomyocytes were purified using the differential adhesion method. Isolated cardiomyocytes were plated in a 24-well plate (Corning, NY, New York, USA) at a density of 25,000 cells/cm² in Dulbecco's modified Eagle's medium (DMEM; Thermo Fisher Scientific, Waltham, MA, USA) containing 4.5 g/L glucose and supplemented with 10% fetal bovine serum (FBS; Thermo Fisher Scientific) and 1% penicillin–streptomycin solution (Thermo Fisher Scientific). The cells were cultured at 37 °C in a humidified atmosphere containing 5% CO₂.

Cell treatment and transfection

OGD was achieved by culturing cells for 12 h in glucose-free DMEM without FBS in a tri-gas incubator (Heal Force, Shanghai, China) saturated with 1% O₂/5% CO₂/94% N₂ at 37 °C for oxygen deprivation. For cell treatment, AA (Sigma-Aldrich, St. Louis, MS,

USA) was dissolved in 5% DMSO and then added to the medium at different concentrations (2, 10, 20, and 50 μmol/L) before OGD. A phosphoinositide 3-kinase (PI3K) inhibitor LY294002 (20 μmol/L; MedChemExpress, Monmouth Junction, NJ, USA) and an Akt inhibitor GSK690693 (10 μmol/L; MedChemExpress) were added to DMEM for 12 h prior to the OGD process. The lentiviral short hairpin RNAs (shRNAs) targeting mice STBD1 and AMPK were purchased from Open Biosystems (Lafayette, CO, USA). To interfere with the expression of STBD1 and AMPK, shSTBD1 and shAMPK were transfected in accordance with the manufacturer's protocol. After 24 h of incubation, the transfection medium was removed, and the cells were harvested for further analysis.

Cell viability and lactate dehydrogenase release assay

Cardiomyocytes were seeded in 96-well plates at a concentration of 1 × 10⁴ cells/mL. Cell viability was detected using a Cell Counting Kit-8 Kit (CCK-8; Dojindo, Tokyo, Japan). Absorbance at 450 nm was measured using a microplate reader (BioTek Synergy 2; Winooski, VT, USA). The mean optical density (OD) measurements from the indicated groups were used to calculate the percentage of cell viability. Lactate dehydrogenase (LDH) release from cardiomyocytes into the medium was assessed using an LDH Cytotoxicity Assay Kit (Roche, Basel, Switzerland) in accordance with the manufacturer's instructions.

High-performance liquid chromatography analysis

ATP and phosphocreatine (PCr) levels in OGD cardiomyocytes and ischemic heart tissue were measured using a high-performance liquid chromatography (HPLC) system (SIL-20A; SHIMADZU, Kyoto, Japan) with detection at 205 nm. Briefly, the heart was quickly removed from the anesthetized mouse and the left ventricular wall was collected. Then, the wall was homogenized with pre-cooled 80% methanol, and supernatants were assayed after centrifugation. Similarly, cardiomyocytes were quickly extracted with pre-cooled 80% methanol, and the supernatants were collected after centrifugation. The following chromatographic conditions were used: (1) mobile phase A (10 mmol/L KH₂PO₄, 2.5% acetonitrile, 5.8 mmol/L tetrabutylammonium hydroxide, pH 6.0), (2) phase B (10 mmol/L KH₂PO₄, 25% acetonitrile, 5.8 mmol/L tetrabutylammonium hydroxide, pH 5.5), and (3) reversed phase (250 mm × 4.6 mm × 5 μm C18 column). ATP and PCr concentrations were determined by dividing the peak area of the samples by the corresponding standard product.

Mitophagic activity detection

A canonical double transfection-based method was used to monitor the mitophagy in cardiomyocytes [22, 23]. Briefly, neonatal cardiomyocytes were transfected with adeno-associated virus containing GFP-LC3-II (Hanbio Inc., Shanghai, China). For Mito-DsRed delivery, the Mito-DsRed DNA sequence was cloned from pDsRed2-Mito (Clontech, 632421) and inserted into the pLVX-puro plasmid (Clontech, 632164) and then transfected into HEK293T cells using a set of plasmids (Clontech, 631247) for lentivirus packaging. After transfection with GFP-LC3-II and Mito-DsRed, the cells were treated and imaged for GFP and DsRed by fluorescence microscopy.

Measurement of extracellular acidification rate

The extracellular acidification rate (ECAR) was measured using a Seahorse XF96 extracellular flux analyzer (Agilent, North Billerica, MA, USA), which reflects the activity of glycolysis. Briefly, cardiomyocytes were seeded in 96-well assay plates at 8 × 10³ cells/well and incubated at 37 °C before analysis. ECAR was recorded immediately after completing OGD. The unit for ECAR was mpH/min.

Animal experiments

Adult C57BL/6 mice (weighing 20–25 g and aged 6–8 weeks) were obtained from Shanghai Model Organisms (Shanghai, China) and cared for in accordance with the Guide for the Care and Use of Laboratory Animals published by the National Institutes of Health (8th

Edition, 2011; Bethesda, MD, USA). Animal procedures were approved by the Tongji University Committee on Animal Care (Shanghai, China). All experiments conformed to the international guidelines on the ethical use of animals. AA was dissolved in 5% dimethyl sulfoxide (DMSO) to form a solution of 500 mg/mL, and then diluted to a volume of 0.5 mL with a specific concentration according to different dosage gradient groups (5, 25, 50, and 125 mg·kg⁻¹·d⁻¹). The AA solution was administered orally to the mice using an intragastric tube on a daily basis for 7 consecutive days after the surgery.

MI models were established surgically by ligation of the left anterior descending (LAD) coronary artery in anesthetized mice as previously described [24]. Briefly, the mice were placed in an induction chamber; they received 2% isoflurane, and were then connected to a small rodent ventilator. Afterward, the chest was opened to expose the heart, left auricle, and LAD. The LAD was permanently ligated with an 8-0 nylon suture, and the chest cavity was closed. After reinstallation of spontaneous respiration, the mice were extubated and allowed to recover from anesthesia. Sham-operated mice underwent the same procedure, excluding LAD ligation. The mice received intraperitoneal injections of buprenorphine (0.1 mg/kg) every 12 h for up to three days and intraperitoneal injections of carprofen (5 mg/kg) every 12 h for up to one day after the surgery.

The following studies were conducted. Study 1: The mice were divided into Sham, MI, MI + DMSO, and MI + AA (5, 25, 50, and 125 mg·kg⁻¹·d⁻¹) groups (*n* = 10). The mice were euthanized seven days after MI, and the hearts were harvested. Study 2: The subgroups were the same as in Study 1 (*n* = 8–10). After completing the echocardiographic examination, the mice were sacrificed 28 days after MI for further analysis. Study 3: The survival curves of Sham, MI, MI + DMSO, and MI + AA (25 mg·kg⁻¹·d⁻¹) groups (*n* = 16–25) up to eight weeks after surgery were recorded.

Determination of myocardial infarct size

Myocardial infarct size at seven days after MI was evaluated using 2,3,5-triphenyltetrazolium chloride (TTC) staining. The left ventricle was isolated and cut into 4-mm slices perpendicular to the axis of the LAD, from the base to the apex. Slices were immediately immersed in 1% TTC (pH 7.4) at 37 °C in the dark for 10 min to distinguish the infarcted tissue from viable myocardium. Infarct size (fibrosis area) of the heart at 28 days after MI was determined using the Masson Trichrome Stain Kit (G1340; Solarbio, Beijing, China) in accordance with the manufacturer's instructions. Infarct size was calculated as a percentage of the left ventricle.

Evaluation of animal cardiac function

The cardiac function in the mice was verified by echocardiography 28 days post-MI. Two-dimensional-guided M-mode echocardiography was used to determine left ventricular chamber volume at systole and diastole and contractile parameters such as left ventricular end-diastolic dimension (LVEDD), left ventricular end-systolic dimension (LVESD), left ventricular end-diastolic volume (LVEDV), and left ventricular end-systolic volume (LVESV). Left ventricular fractional shortening (LVFS) was calculated as follows: FS (%) = (LVEDD – LVESD)/LVEDD × 100%. Left ventricular ejection fraction (LVEF) was derived as follows: EF (%) = (LVEDV – LVESV)/LVEDV × 100%. All measurements were based on the average of at least three cardiac cycles.

Immunofluorescence

Cardiomyocytes or cardiac tissue were fixed for 15 min in 4% paraformaldehyde at room temperature and then permeabilized for 20 min with 0.25% Triton X-100 at room temperature. After blocking in 4% bovine serum albumin for 7 min at room temperature, the sections were incubated with primary antibodies (1:100 cardiac troponin I [cTnI] and 1:100 CD31; Abcam, Cambridge, MA, USA) and subsequently with 1:500 secondary antibody conjugated to Alexa Fluor-488 and Alexa Fluor-549 (Life Technologies, Waltham, MA, USA).

The TUNEL assay (Roche) and wheat germ agglutinin (WGA; Sigma) staining were performed according to the manufacturer's instructions. After final washing, the coverslips were mounted on the slides using 50% glycerin, and the nuclei were further stained with DAPI (Beyotime, Jiangsu, China). The tissues and cells were observed using a confocal laser scanning microscope (Olympus, Tokyo, Japan), and analysis was performed by Image-Pro Plus (Media Cybernetics Inc., Bethesda, MA, USA).

Transmission electron microscopy

Heart tissue samples were fixed in 2.5% glutaraldehyde overnight. Subsequently, they were incubated with 1% osmium tetroxide for 2 h in dark. After washing in distilled water, the samples were incubated with 2% uranyl acetate for 2 h at room temperature and then dehydrated in an ethanol concentration gradient. Finally, the samples were embedded in molds with fresh resin. Ultrathin sections were obtained using the EM UC7 ultramicrotome (Leica, Solms, Germany), stained with lead citrate, and examined using Tecnai G2 T12 (FEI Co., Hillsboro, OR, USA).

Western blot analysis

Heart tissue protein was extracted from the left ventricular myocardium using a lysis buffer (100 mmol/L Tris-HCl, 4% SDS, 20% glycerine, 200 mmol/L DTT, phosphatase, and protease inhibitors, pH 6.8). For whole cell lysates, cells were lysed with the Cell Total Protein Extraction Kit (Sangon, Shanghai, China). Protein concentrations were measured using a bicinchoninic acid (BCA) assay kit (Beyotime) in accordance with the manufacturer's instructions. Proteins were resolved by 8%–12% sodium dodecyl sulfate-polyacrylamide gel electrophoresis (SDS-PAGE) and electrotransferred to nitrocellulose membranes (Millipore, Darmstadt, Germany). The membranes were probed overnight at 4 °C with the following primary antibodies: STBD1 (1:1000, 11942-1-AP; Proteintech, Rosemont, IL, USA), GBARAP1 (1:1000, 26632; Cell Signaling, Beverly, MA, USA), phosphorylated Akt (p-Akt) at Ser473 (1:1000, 4060; Cell Signaling), Akt (1:1000, 9272; Cell Signaling), phosphorylated glycogen synthase kinase 3 beta (p-GSK3β) at Ser9 (1:1000, 9323; Cell Signaling), GSK3β (1:1000, 9832; Cell Signaling), LC3-I/II (1:1000, 4108; Cell Signaling), p-AMPKα at Thr172 (1:1000, 2535; Cell Signaling), AMPKα (1:1000, 5832; Cell Signaling), or GAPDH (1:5000, 60004-1-Ig; Proteintech). After washing, the membranes were incubated with secondary antibody for 2 h at room temperature. Finally, proteins were detected by the Odyssey Infrared Imaging System (Li-Cor, Lincoln, NE, USA) and quantified using ImageJ software (NIH). For all Western blot analyses, unless specifically noted, protein levels were calculated from the ratio of corresponding protein/GAPDH.

Quantitative PCR

Quantitative PCR (qPCR) was used to determine the mRNA level of AMPKα both in cardiomyocytes and in mouse heart tissue. Total RNA was extracted using TRIzol reagent (Thermo Fisher Scientific). The RNA (1000 nmol) was subjected to reverse transcription using the PrimeScript RT Reagent Kit with gDNA Eraser (TaKaRa, Dalian, China). Then, 20-μL reactions with primers (GENEWIZ, South Plainfield, NJ, USA) were detected by Light Cycler 480II (Roche) using SYBR Green PCR Master Mix (Thermo Fisher Scientific). Relative quantitative analysis of the change in expression levels was obtained using the $\Delta\Delta$ CT method and normalized to GAPDH. The primer sequences are as follows:

5'-GGCCTCACCTGAGAGAGTA-3' (AMPKα forward),
5'-TCACAGGGTTCTTCCTTCGC-3' (AMPKα reverse),
5'-GGAGCGAGACCCCACTAACAT-3' (GAPDH forward),
5'-ACATACTCAGACCCGGCCTC-3' (GAPDH reverse).

Co-immunoprecipitation

The whole proteins from cardiomyocytes were extracted using lysis buffer for immunoprecipitation. The lysates were centrifuged, and

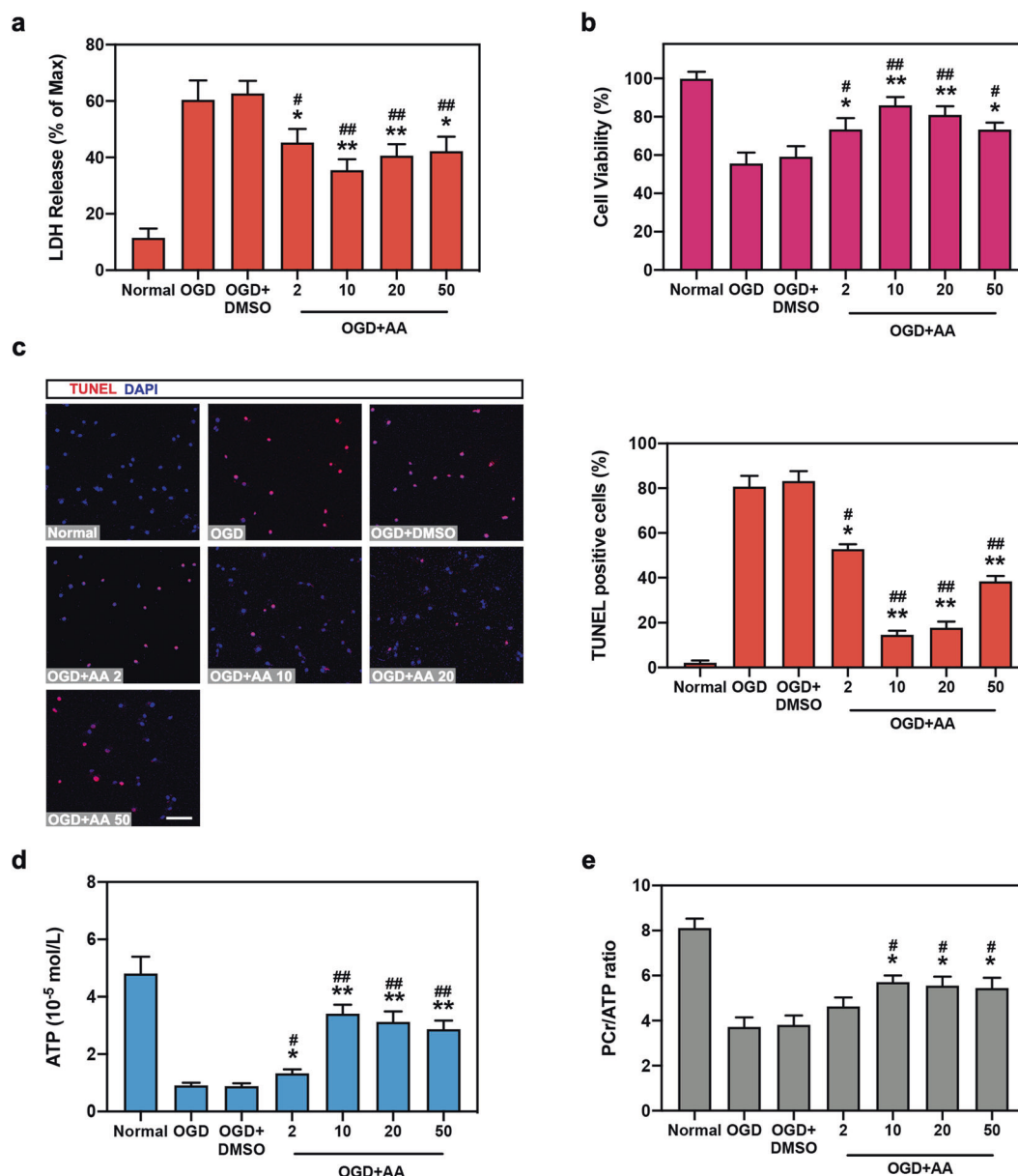


Fig. 1 Asiatic acid (AA) protects oxygen-glucose deprivation (OGD) cardiomyocytes in vitro. Isolated neonatal mouse cardiomyocytes were divided into normal group, OGD for 12 h group, OGD + DMSO group, and OGD + concentration gradient of AA (2, 10, 20, and 50 $\mu\text{mol/L}$) group. **(a, b)** Lactate dehydrogenase (LDH) release **(a)** and cell viability **(b)** were analyzed in cardiomyocytes. **(c)** The TUNEL assay was performed and analyzed in isolated mouse cardiomyocytes. Bar: 50 μm . **(d, e)** ATP **(d)** and phosphocreatine (PCr) levels were measured by high-performance liquid chromatography (HPLC) analysis, and the ratio of PCr/ATP **(e)** was calculated. $n = 5\text{--}6$ independent experiments. * $P < 0.05$, ** $P < 0.01$ vs. OGD group, # $P < 0.05$, ## $P < 0.01$ vs. OGD + DMSO group. Data are presented as the mean \pm SEM.

protein concentrations were measured using the BCA assay. A part of the supernatant was used as input control, while the rest was immunoprecipitated overnight at 4 $^{\circ}\text{C}$ by gently rocking with anti-STBD1 antibody. Approximately 4 μL antibody was used (400 μg total protein). Protein A/G agarose beads (Santa Cruz, Dallas, TX, USA) were added to the immunoprecipitates for 2 h with gentle shaking at room temperature. The precipitated proteins were washed three times with lysis buffer and boiled with 5 \times loading buffer, followed by Western blot analysis as previously described. Rabbit normal IgG (Santa Cruz) served as the negative control.

Statistical analysis

Data are expressed as the mean \pm standard error of the mean (SEM). Statistical analyses were performed using SPSS 24.0 (IBM, Armonk, NY, USA). Significant differences between means were analyzed using the

unpaired Student's *t*-test or one-way analysis of variance followed by Tukey's *post hoc* test. Analysis of survival was performed using log-rank (Mantel-Cox and Gehan-Breslow-Wilcoxon) tests applied to Kaplan-Meier survival curves. $P < 0.05$ was considered statistically significant.

RESULTS

AA attenuates ischemic myocardial injury and promotes energy metabolism

We first determined the effects of AA on OGD cardiomyocytes. As shown in Figs. 1a and 1b, 2–50 $\mu\text{mol/L}$ AA significantly decreased LDH release and upregulated cell viability compared with the OGD + DMSO or OGD groups. Importantly, 10 $\mu\text{mol/L}$ AA showed the best cytoprotective effects on OGD cardiomyocytes. The TUNEL assay

further indicated that 10 $\mu\text{mol/L}$ AA had the strongest cellular antiapoptotic effects (Fig. 1c). Next, energy metabolism was investigated in OGD cardiomyocytes to further determine the cardioprotective roles of AA. The PCr/ATP ratio is an important indicator for myocardial energetic reserve, and it is reduced in patients with severe coronary artery disease and acute MI [25]. AA concentration starting from 10 $\mu\text{mol/L}$ significantly increased the ATP level and PCr/ATP ratio, suggesting a higher energy metabolism level and energy reserve (Fig. 1d, e). In addition, DMSO did not show any effect on cell function under normal and OGD conditions (Fig. S1).

Next, dose gradients of AA (5, 25, 50, and 125 $\text{mg}\cdot\text{kg}^{-1}\cdot\text{d}^{-1}$) were used to determine the effective dose of AA in vivo. As shown in Fig. 2a, oral administration of AA starting from 5 $\text{mg}\cdot\text{kg}^{-1}\cdot\text{d}^{-1}$ relieved cellular apoptosis compared with the MI (seven days) or the MI + DMSO groups, and 25 $\text{mg}\cdot\text{kg}^{-1}\cdot\text{d}^{-1}$ showed the best cardioprotective effect. Also, acute cardiac infarct size determined by TTC staining was markedly reduced in the MI + 25 $\text{mg}\cdot\text{kg}^{-1}\cdot\text{d}^{-1}$ AA group (Fig. 2b). In addition, the long-term protective effects of AA on MI were explored. As shown in Figs. 2c and 2d, AA ≥ 5 $\text{mg}\cdot\text{kg}^{-1}\cdot\text{d}^{-1}$ improved the LVEF and fractional shortening (FS) compared with the chronic MI (28 days) and MI + DMSO groups. Especially, 25 $\text{mg}\cdot\text{kg}^{-1}\cdot\text{d}^{-1}$ AA treatment in MI mouse showed the best cardioprotective effects on improving EF and FS. Masson trichrome staining revealed reduced cardiac infarct size (fibrotic area) of chronic MI in 25 $\text{mg}\cdot\text{kg}^{-1}\cdot\text{d}^{-1}$ AA-treated mouse myocardium (Fig. 2e). In addition, cardiac myocyte hypertrophy after chronic MI was alleviated by AA treatment (25 $\text{mg}\cdot\text{kg}^{-1}\cdot\text{d}^{-1}$) (Fig. 2f). However, no differences in cardiac angiogenesis were observed between the AA-treated group (25 $\text{mg}\cdot\text{kg}^{-1}\cdot\text{d}^{-1}$) and control (Fig. 2g). The survival rate was significantly higher in the MI mice that had received 25 $\text{mg}\cdot\text{kg}^{-1}\cdot\text{d}^{-1}$ AA than in the MI (56 days) and MI + DMSO groups (Fig. 2h). In addition to the in vitro promotion of energy metabolism, AA treatment restored the ATP level and PCr/ATP ratio in the acute (7 days, Fig. 2i, j) or chronic MI myocardium (28 days; Fig. 2k, l). These results demonstrated that AA could modulate the acute and chronic cardioprotective and energy metabolic effects on MI cardiomyocytes both in vitro and in vivo. An AA concentration of 10 $\mu\text{mol/L}$ AA in vitro and a dose of 25 $\text{mg}\cdot\text{kg}^{-1}\cdot\text{d}^{-1}$ in vivo showed the best protective effects and were used in subsequent studies.

AA promotes mitophagy in OGD cardiomyocytes

As AA is involved in the regulation of cellular energy metabolism, we next evaluated the effects of AA on mitophagy, an important autophagic process that maintains energy homeostasis in the MI heart [18]. Transmission electron microscopy (TEM) revealed that the mitochondria in myocytes of the MI group were swollen dramatically compared with the Sham group, revealing serious myocardial injury, while relieved mitochondrial edema and increased number of mitophagosomes (red arrows) were observed in the MI + AA group (Fig. 3a). Western blotting demonstrated that the autophagic indicator, LC3-II expression, was upregulated in AA-treated OGD cardiomyocytes compared with the OGD and OGD + DMSO groups (Fig. 3b). Congruously, the fluorescence results also revealed a significant increase in LC3-II positive puncta in AA-treated OGD cardiomyocytes (Fig. 3c, d). Additionally, the co-localization of LC3-II and mitochondria significantly increased in OGD cardiomyocytes after AA treatment, confirming the increased mitophagic activity in this in vitro model (Fig. 3c, e). These results revealed that AA may be responsible for the promoted mitophagy in ischemic myocardium and cardiomyocytes.

AMPK pathway is involved in AA-induced mitophagy

AMPK is a vital energy and mitophagic modulator of most tissue cells, especially under hypoxic environments [26]. Therefore, we investigated AMPK activation in OGD cardiomyocytes and MI cardiac tissue. We found upregulated expression of p-AMPK α at threonine 172 in OGD cardiomyocytes, and AA treatment further improved the activation of AMPK (Fig. 4a). In addition, there was no significant difference in AMPK α mRNA expression in cardiomyocytes between

the AA-treated group and controls (Fig. 4b). Similar results were also observed in the myocardial tissue (Fig. 4c, d). To determine whether AMPK is associated with AA roles in mitophagy, shRNA was used to inhibit AMPK expression (Fig. 4e, f). As expected, AMPK deletion completely reversed the increased LC3-II expression in AA-treated OGD cardiomyocytes (Fig. 4g) and inhibited the increased mitophagic activity induced by AA (Fig. 4h–j). These results suggest that AMPK-regulated mitophagy may be one of the mechanisms by which AA protects the ischemic heart.

AA treatment upregulates glycolipophagy in OGD cardiomyocytes

The regulation of glycogen degradation and utilization (glycolipophagy) in AA-treated ischemic myocardium and cardiomyocytes was also investigated. As shown in Fig. 5a, glycoliposomes sequestering the glycogen particles were observed in the myocardium of the MI + AA group (orange arrows). Co-immunoprecipitation was performed to explore the effects of the combination of STBD1 and GABARAPL1, which is critical for the delivery of glycogen to lysosomes in the autophagic pathway [20]. The expression of both STBD1 and GABARAPL1 was elevated in the AA-treated OGD group compared with the OGD and OGD + DMSO group (cell lysates) (Fig. 5b). Similar results were observed by pulling down STBD1. The binding and interaction of STBD1 and GABARAPL1 were significantly enhanced in the OGD + AA group, indicating promoted glycolipophagy. To evaluate the utilization of glucose produced by glycolipophagy, ECAR was analyzed using the Seahorse XF96 extracellular flux analyzer to determine the glycolytic activity in cardiomyocytes (Fig. 5c). Glycolysis was significantly promoted in AA-treated OGD cardiomyocytes compared with OGD and OGD + DMSO groups. Furthermore, to evaluate the relationship between glycolipophagy and the protective effects of AA, shRNA inhibiting STBD1 expression was constructed to decrease STBD1 expression and STBD1-GABARAPL1 binding in OGD cardiomyocytes (Fig. 5d); we found that STBD1 depletion significantly abolished the promoted ECAR in AA-treated cardiomyocytes (Fig. 5c).

PI3K/Akt pathway is responsible for AA-induced glycolipophagy

The expression and interaction of STBD1 and GABARAPL1 are associated with the activation of PI3K/Akt axis [27–29]. Thus, the downstream mechanisms of glycolipophagy induced by AA in OGD cardiomyocytes were determined. The protein expression of phosphorylated Akt at serine 473 and phosphorylated GSK3 β at serine 9 were markedly elevated compared with the OGD and OGD + DMSO groups (Fig. 6a, b). Importantly, the specific PI3K inhibitor LY294002 and Akt activation inhibitor GSK690693 abolished the effects of AA on upregulation of STBD1 and GABARAPL1 expression (Fig. 6c). In addition, the interaction between STBD1 and GABARAPL1 was also inhibited. Inhibition of PI3K/Akt signaling also abolished the increased glycolysis achieved by AA (Fig. 6d).

Glycolipophagy and mitophagy are key factors for AA to protect ischemic cardiomyocytes

Finally, we determined whether AMPK-regulated mitophagy and PI3K/Akt-regulated glycolipophagy are involved in AA-mediated cardioprotection and energy metabolism under OGD. Inhibition of the PI3K/Akt pathway (LY294002 and GSK690693) significantly elevated LDH release and decreased cell viability compared with the AA group (Fig. 7a, b). Consistently, depletion of AMPK expression (shAMPK) also abolished the protective roles of AA. Importantly, simultaneous suppression of PI3K/Akt and AMPK (LY294002 + shAMPK or GSK690693 + shAMPK) further aggravated the AA-treated cardiomyocyte injury compared with single PI3K/Akt inhibition or AMPK inhibition. Similar results were also observed in the TUNEL assay and in energy metabolic analysis in vitro (Fig. 7c–e). No significant effects of single-use of shAMPK and PI3K/Akt inhibitors on cell function were observed (Fig. 7 and Fig. S1). These results reveal that mitophagy regulated by AMPK and glycolipophagy modulated by PI3K/Akt signaling are both involved in AA-induced myocardial protection and energy metabolism.

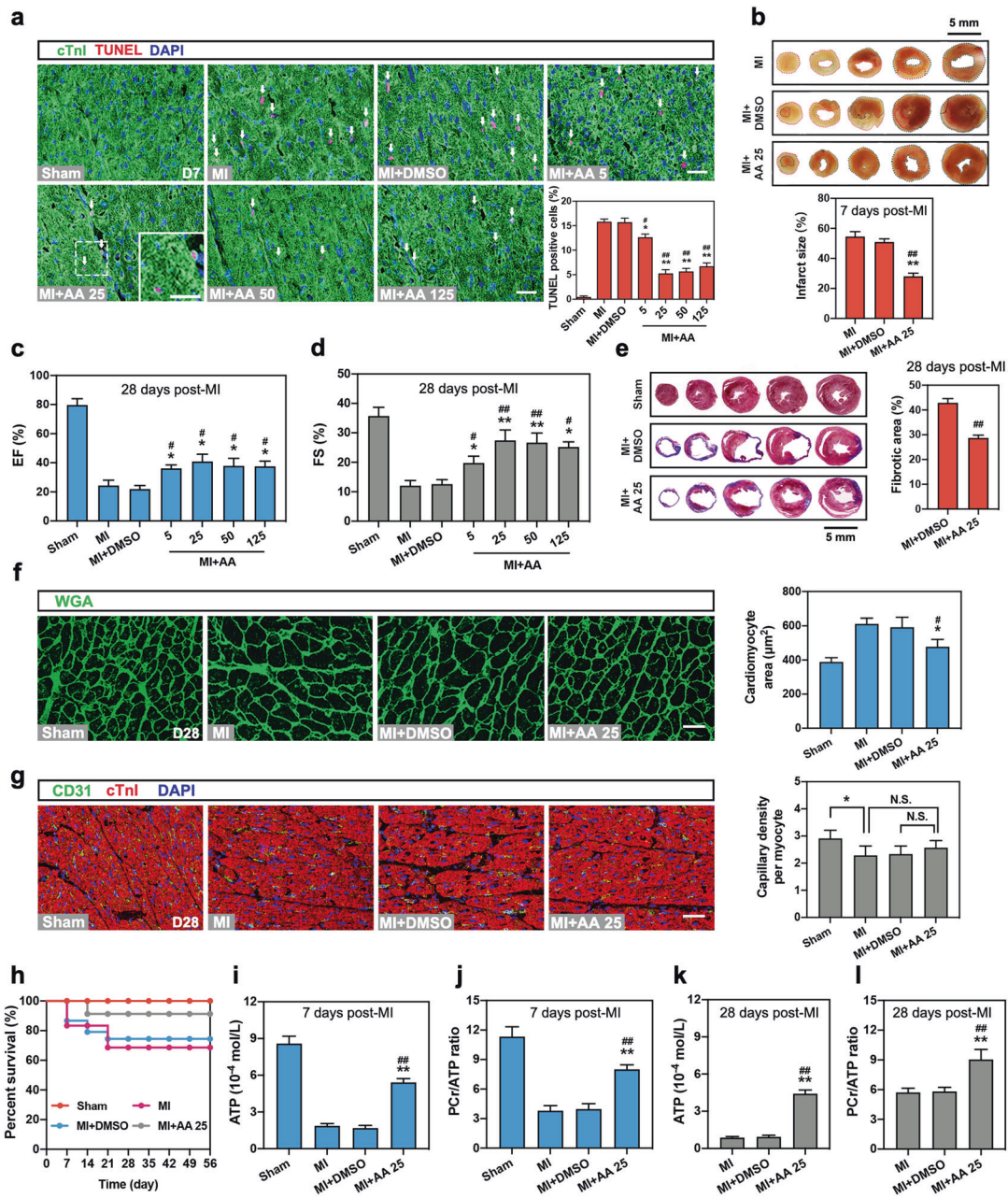


Fig. 2 AA reduces ischemic myocardial injury and improves cardiac function in vivo. The mice were divided into Sham, myocardial infarction (MI) (7 or 28 days), MI + DMSO, and MI + dose gradient of AA (5, 25, 50, and 125 mg·kg⁻¹·d⁻¹) groups. **a** Representative images of TUNEL assay and statistical analysis in the border zone of mouse heart 7 days after MI, *n* = 4 mice per group. Bar: 25 μm. White arrows indicate the TUNEL-positive nuclei; the box indicates the area enlarged on the lower left. **b** Representative images of the cross-sections from the apex to the vicinity of the ligation site and statistical analysis of cardiac infarct size in 2,3,5-triphenyltetrazolium chloride (TTC)-stained MI (7 days) heart, *n* = 6 mice per group. The red dotted area indicates the infarct area, and the black dotted area indicates the normal area, bar: 5 mm. **c, d** Measurement of left ventricular ejection fraction (LVEF) (**c**) and fractional shortening (LVFS) (**d**) in mice of the Sham group, MI group (28 days), MI + DMSO group, and MI + dose gradient of AA (5, 25, 50, and 125 mg·kg⁻¹·d⁻¹) group by echocardiography, *n* = 8–10 mice per group. **e** Representative images and analysis of infarct size in MI (28 days) heart with Masson trichrome staining, *n* = 6 mice per group. Bar: 5 mm. **f, g** Representative images and analysis of wheat germ agglutinin (WGA) staining (**f**) and CD31 staining (**g**) in the border zone of heart tissue 28 days following MI, *n* = 6 mice per group. Bar: 25 μm. **h** Survival analysis was performed in neonatal mice from seven days to 56 days post-MI, *n* = 16–25 mice per group. **i, j** ATP (**i**) and PCr levels in the border zone of mouse heart were measured by HPLC analysis, and the ratio of PCr/ATP (**j**) was calculated seven days post-MI, *n* = 5 mice per group. **k, l** ATP level (**k**) and PCr/ATP ratio (**l**) in the border zone of myocardium 28 days following MI, *n* = 5 mice per group. **P* < 0.05, ***P* < 0.01 vs. MI group or indicated group, ###*P* < 0.05, ###*P* < 0.01 vs. MI + DMSO group. N.S. indicates no significance. Data are presented as the mean ± SEM.

DISCUSSION

Myocardial infarction is the leading cause of human death worldwide. Altered mitochondrial function and energy metabolism in cardiomyocytes contribute to the pathophysiology of heart

injury caused by MI [3]. However, at present, drugs for myocardial infarction, based on ameliorating energy imbalance, are scarce. In this study, we demonstrated that 25 mg·kg⁻¹·d⁻¹ AA in vivo and 10 μmol/L AA in vitro significantly promoted cardiac function and

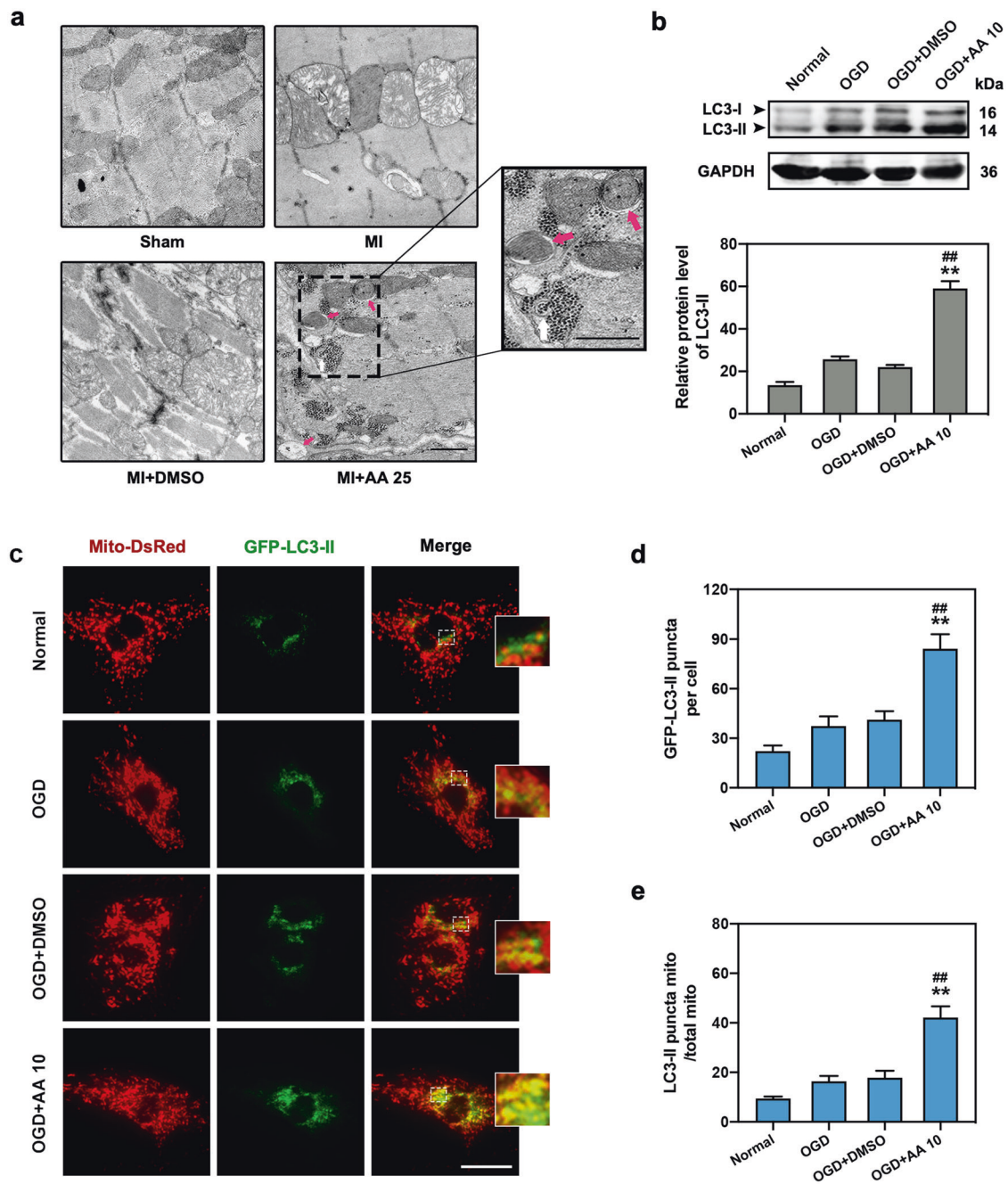


Fig. 3 AA increases ischemic cardiomyocyte mitophagy. The dose of AA was 25 mg·kg⁻¹·d⁻¹ (AA 25) in vivo and 10 μmol/L (AA 10) in vitro. **a** Transmission electron micrograph of mitophagosomes enveloping mitochondria (red arrows) in the border zone of mouse MI (7 days) myocardium with AA 25 treatment; the box indicates the area enlarged on the lower right. Swollen mitochondria were observed in MI and MI + DMSO group, whereas mitochondrial damage was significantly alleviated in AA 25 group, bar: 500 nm. **b** Western blot and quantitative analysis of light chain 3 (LC3)-II expression in normal, OGD, OGD + DMSO, and OGD + AA 10-treated isolated cardiomyocytes, *n* = 4 independent experiments. **c–e** Representative images of isolated cardiomyocytes transfected with GFP-LC3-II adeno-associated virus and Mito-DsRed lentivirus (**c**); the number of LC3-II puncta (**d**) and the ratio of LC3-II positive mitochondria/total mitochondria (**e**) were determined, *n* = 5 independent experiments. Bar: 200 μm. ^{**}*P* < 0.01 vs. OGD group, ^{##}*P* < 0.01 vs. OGD + DMSO group. Data are presented as the mean ± SEM.

energy metabolism, and reduced infarct size and cell injury; that the AA-induced cardioprotective effects on ischemic myocardium and cardiomyocytes were related to the enhanced mitophagy and glycopyagy flux; that AMPKα activation was involved in AA-mediated mitophagy in MI; and that STBD1/GABARAPL1 binding and PI3K/Akt axis were responsible for glycopyagy regulated by AA in the ischemic myocardium and cardiomyocytes (Fig. 8). These findings extend previous knowledge and provide insights

into the mechanisms underlying the cardioprotection conferred by AA, supporting the fact that AA may be a drug candidate for the treatment of ischemic heart disease.

In the infarcted myocardium, mitochondrial damage results in decreased ATP and PCr level and lower myocardial energy reserve [4]. Ameliorating the energy imbalance may increase the survival rate of cardiomyocytes in the infarct zone, allowing more cells to recover after the blood supply is restored. Various molecular

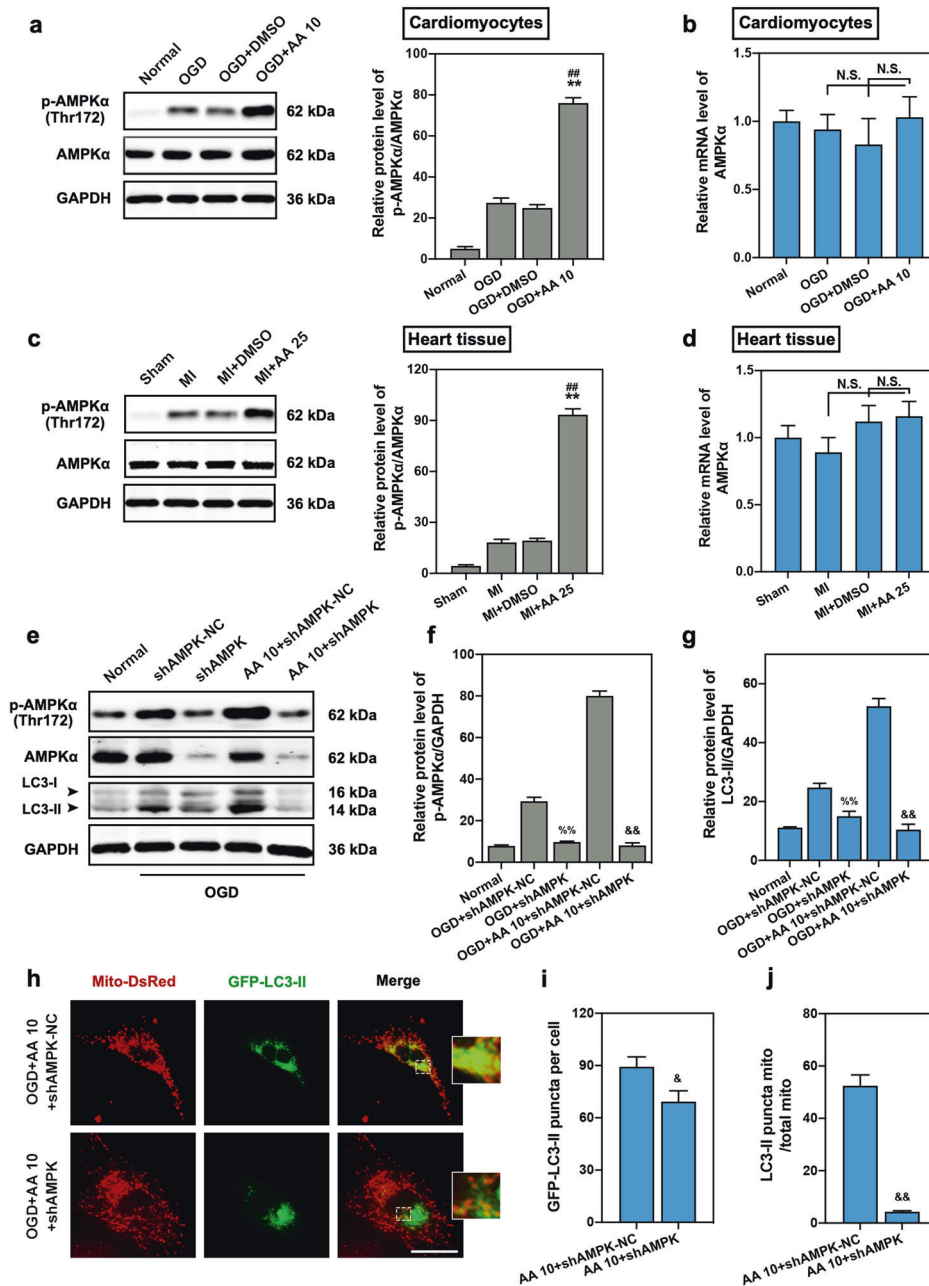


Fig. 4 Activation of the AMP-activated protein kinase (AMPK) signaling pathway is responsible for AA-induced mitophagy. The dose of AA was 25 mg·kg⁻¹·d⁻¹ (AA 25) in vivo and 10 μ mol/L (AA 10) in vitro. **a** Western blotting and quantitative analysis for AMPK α phosphorylation in isolated cardiomyocytes from mice (normal, OGD, OGD + DMSO, OGD + AA 10), $n = 4$ independent experiments. **b** qPCR analysis of AMPK α mRNA expression in isolated cardiomyocytes, $n = 4$ independent experiments. **c** Western blotting and quantitative analysis for AMPK α phosphorylation in the border zone of cardiac tissue (Sham, MI, MI + DMSO, MI + AA 25), $n = 4$ mice per group. **d** qPCR analysis of AMPK α mRNA expression in cardiac tissue, $n = 4$ mice per group. **e** Western blotting for p-AMPK α and LC3-II expression in isolated cardiomyocytes treated with short hairpin RNA targeting AMPK-negative control (shAMPK-NC), shAMPK, and/or AA, and then subjected to OGD insult. **f**, **g** Quantitative analysis of p-AMPK α (**f**) and LC3-II (**g**) expression in isolated cardiomyocytes, $n = 4$ independent experiments. **h–j** Representative images of transfected cardiomyocytes (**h**); the number of LC3-II puncta (**i**) and the ratio of LC3-II positive mitochondria/total mitochondria (**j**) were calculated, $n = 5$ independent experiments. Bar: 200 μ m. ^{**} $P < 0.01$ vs. OGD or MI group, ^{##} $P < 0.01$ vs. OGD + DMSO or MI + DMSO group, ^{%%} $P < 0.01$ vs. OGD + shAMPK-NC group, [&] $P < 0.05$, ^{&&} $P < 0.01$ vs. OGD + AA 10 + shAMPK-NC group; N.S. indicates no significance. Data are presented as the mean \pm SEM.

compounds and proteins have ameliorated the energy metabolism disorder in infarcted myocardium, which provides new insights into MI treatment [30–32]. Our research revealed that AA, a pentacyclic triterpene, improved mitophagy- and glycophyagy-related energy metabolism of ischemic cardiomyocytes and reduced the infarct

size, thereby expanding the possibilities of AA application in the field of MI. In addition, our study also suggests that the optimal concentration and dosage of AA to protect mouse ischemic cardiomyocytes in vitro and in vivo are 10 μ mol/L and 25 mg·kg⁻¹·d⁻¹, respectively. Compared with the low-dose group, an

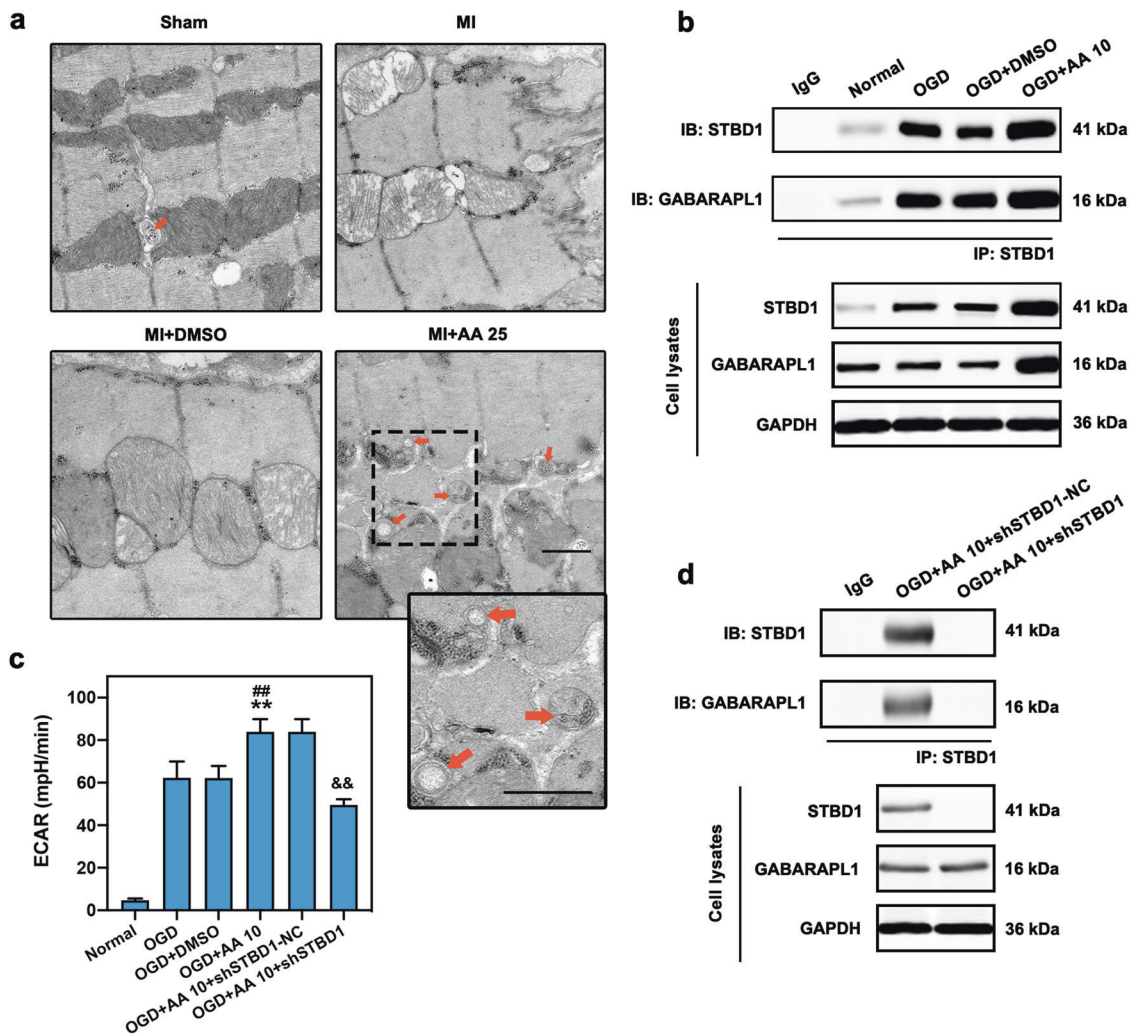


Fig. 5 Increased glycophyagy is observed in OGD cardiomyocytes with AA treatment. The dose of AA was 25 mg·kg⁻¹·d⁻¹ (AA 25) in vivo and 10 μmol/L (AA 10) in vitro. **a** Electron micrograph of glycophyagosomes (orange arrows) in mouse MI (seven days) myocardium with AA 25 treatment; the box indicates the area enlarged on the lower right. Free glycogen particles were observed between myofibrils and mitochondria, and some glycogen particles were seen isolated in a glycophyagosome, bar: 500 nm. **b** Isolated cardiomyocytes were treated with OGD, OGD + DMSO or OGD + AA 10, then immunoprecipitated with starch binding domain protein 1 (STBD1) antibody. STBD1 and GABA type A receptor-associated protein-like 1 (GABARAPL1) expression were determined using anti-STBD1 and anti-GABARAPL1 antibodies. **c** The extracellular acidification rate (ECAR) analysis via Seahorse XF96 extracellular flux analyzer was carried out to determine the glycolytic activity in isolated cardiomyocytes, *n* = 6 independent experiments. **d** Isolated cardiomyocytes were treated with AA 10 and shSTBD1-NC or shSTBD1 and then immunoprecipitated with STBD1 antibody. ***P* < 0.01 vs. OGD group, ##*P* < 0.01 vs. OGD + DMSO group, &&*P* < 0.01 vs. OGD + AA 10 + shSTBD1-NC group. Data are presented as the mean ± SEM. IB immunoblotting, IP immunoprecipitation.

AA concentration higher than 10 μmol/L or 25 mg·kg⁻¹·d⁻¹ showed diminished protective effects on cell apoptosis and energy metabolism, but no toxic effects on cardiomyocytes were observed at high doses. Previous reports revealed that AA reduces ischemic myocardial injury by modulating inflammatory response and glycometabolism [33, 34]. In this study, we elucidated a new mechanism underlying the AA-mediated cardioprotection; specifically, AA improves energy metabolism by regulating mitophagy to maintain mitochondrial function and by modulating glycophyagy to increase glycogen utilization.

Autophagy is a lysosomal degradation pathway that plays an important role in the maintenance of cellular homeostasis and the recycling of energy and material [35]. Although autophagy has been considered a nonselective process, accumulating evidence suggests the existence of selective autophagy through damaged organelles, including mitochondria, endoplasmic reticulum,

ribosomes, and peroxisomes [36, 37]. Among them, mitochondria-specific autophagy, termed mitophagy, has been most extensively studied, and is most closely related to energy homeostasis in ischemic cardiomyocytes [3]. Mitochondrial quality is an important determinant of cell viability, and mitophagy plays a crucial role in this control mechanism. Genetic or pharmacological inhibition of autophagy has been shown to exacerbate myocardial ischemic injury and chronic cardiac remodeling in MI mouse models [38, 39]. Conversely, activation of autophagy limits myocardial damage in response to ischemia and reduces chronic ischemic remodeling and heart failure [39, 40]. However, the excessive activation of mitophagy may weaken its cardioprotective effects due to the loss of mitochondrial quantity and function. Therefore, it is necessary to prevent the overactivation of pharmacological or genetic mitophagy. Our results demonstrated that 10 μmol/L or 25 mg·kg⁻¹·d⁻¹ AA can moderately activate

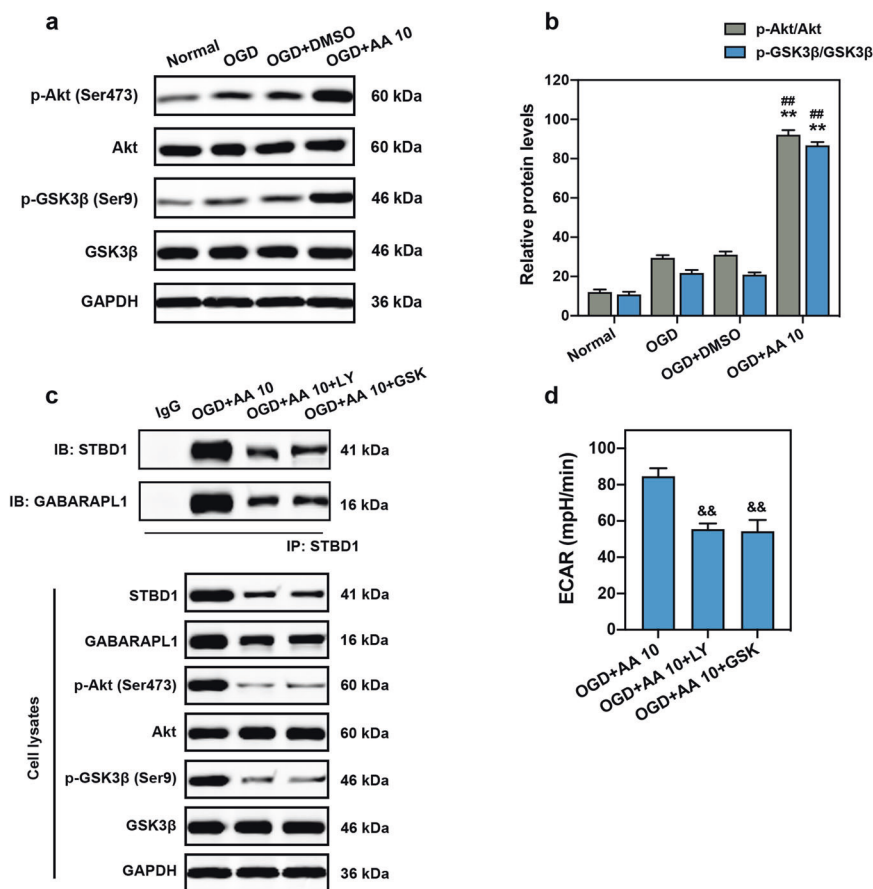


Fig. 6 Phosphoinositide 3-kinase (PI3K)/Akt is involved in AA-induced glycolysis. **a, b** Representative Western blots (**a**) and quantitative analysis (**b**) of Akt and glycogen synthase kinase 3 beta (GSK3β) phosphorylation in isolated cardiomyocyte lysates, $n = 4$ independent experiments. **c** Co-immunoprecipitation of STBD1 and GABARAPL1 in isolated cardiomyocytes treated with AA (10 $\mu\text{mol/L}$; before OGD), PI3K inhibitor LY294002 (LY; 20 $\mu\text{mol/L}$), or Akt inhibitor GSK690693 (GSK; 10 $\mu\text{mol/L}$) and then subjected to OGD. The expression levels of Akt and GSK3β in cell lysates were also verified. **d** ECAR analysis was carried out to determine the glycolytic activity in isolated cardiomyocytes, $n = 6$ independent experiments. $**P < 0.01$ vs. OGD group, $##P < 0.01$ vs. OGD + DMSO group. $\&\&P < 0.01$ vs. OGD + AA 10 + DMSO group. Data are presented as the mean \pm SEM.

mitophagy in ischemic cardiomyocytes, thereby reducing the excessive consumption of intracellular energy and promoting cardiomyocyte survival.

In mammalian cells, several types of autophagy, including mitophagy, are regulated by the AMPK pathway [26]. AMPK can directly phosphorylate ULK1 on Ser467, Ser555, Thr574, and Ser637 [13, 41], and it plays a crucial regulatory role in mitophagy under various conditions [42–44]. In our study, the activation of AMPK increased under ischemic conditions in cardiomyocytes, and p-AMPK α expression was further elevated, indicating enhanced activation of the AMPK signaling pathway in the AA-treated MI heart. Inhibition of AMPK expression abolished all of the effects of AA on mitophagy, indicating that AMPK may be a central regulator connecting AA and mitophagy. LC3, one of the mammalian Atg8 orthologs, is typically used as an indicator of autophagic or mitophagic flux [45, 46]. AMPK is necessary and sufficient for LC3 lipidation (LC3-I to LC3-II) to induce autophagosome formation [15], which is consistent with our findings. However, further studies are needed to clarify the specific mechanism downstream of AMPK in AA-treated ischemic cardiomyocytes.

There have been few studies on glycolysis in myocardial infarction; nevertheless, glycolysis may play an important role in maintaining the energy supply of cardiomyocytes after MI. Cytosolic glycogen is localized in the myocyte subcellular regions, including intramyofibrillar, intermyofibrillar, and subsarcolemmal

compartments [47]. Glycolysis is a glycogen degradation and utilization process, which triggers the liberation of free glucose that can be rapidly utilized by cells with energy requirements [16]. In the setting of a local high demand for glycogen, glycolysis may support the cytosolic machinery and metabolism in the myocardium under ischemic stress. In addition to increased mitophagic levels, an increased number of glycolysosomes was observed, indicating promoted glycolysis. The increased glycolytic level elevates the content of intracellular free glycogen, thereby providing the necessary energy supply for ischemic cardiomyocytes and maintaining their survival. Here, we verified the role of AA in glycolysis through the PI3K/Akt axis. Mechanistically, the interaction of STBD1 and GABARAPL1 and activation of the PI3K/Akt pathway in OGD cardiomyocytes were also enhanced by AA treatment. Furthermore, loss-of-function analysis suggested that the binding of STBD1 and GABARAPL1 was weakened by a PI3K or an Akt inhibitor. These results demonstrated that the PI3K/Akt axis and STBD1-GABARAPL1 interaction are responsible for the effects of AA on glycolysis in OGD cardiomyocytes. In addition, it is intriguing to observe that LY294002 and GSK690693 inhibit the phosphorylation of Akt at the same level, as well as GSK3β, suggesting that Akt and GSK3β may be comparably activated and that the PI3K/Akt/GSK3β axis is responsible for the AA-mediated glycolysis in OGD cardiomyocytes. However, further studies are needed to unravel how GSK3β affects STBD1. Inactivation of PI3K/Akt and/or AMPK also deteriorated cell

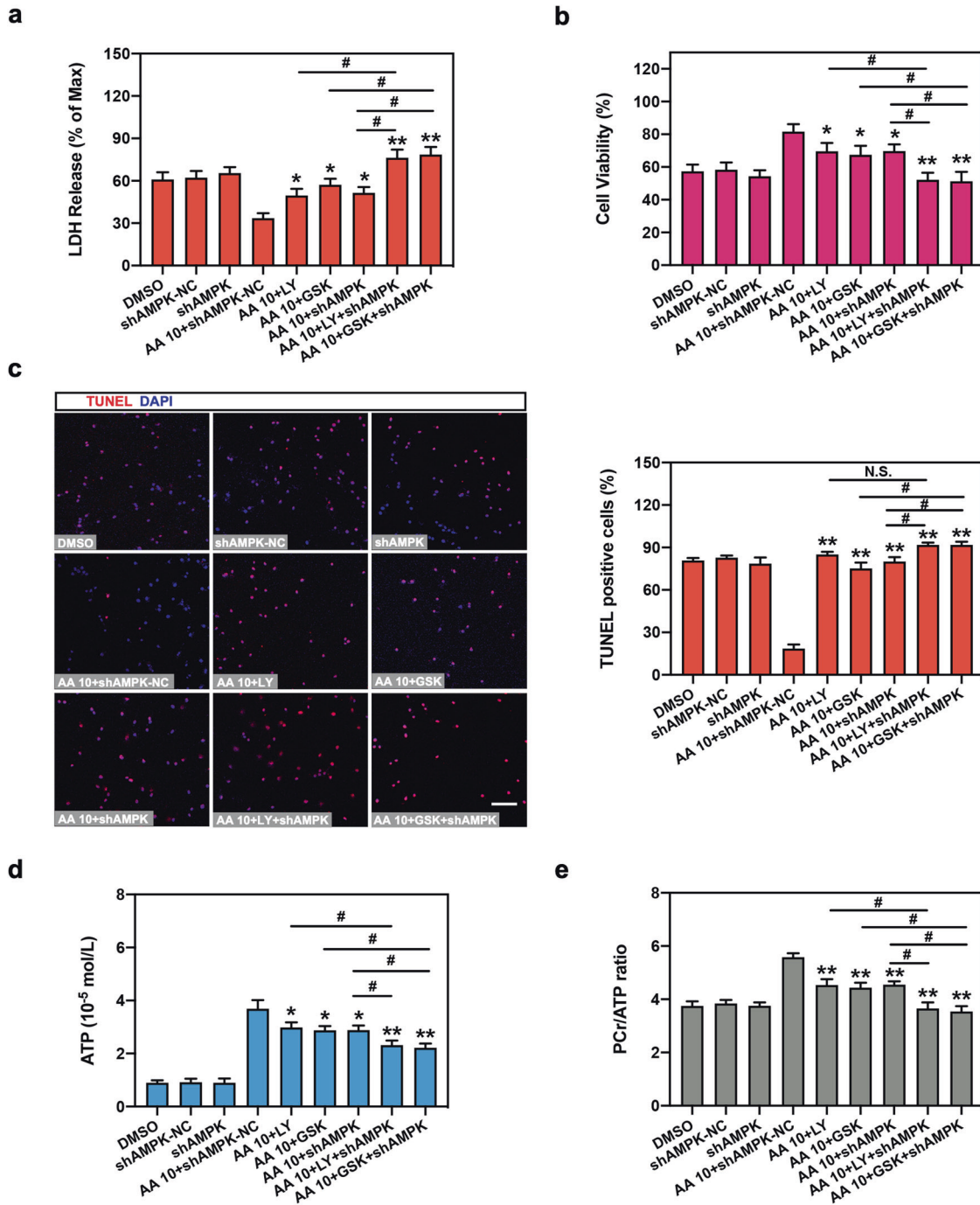


Fig. 7 Glycophagy and mitophagy are critical for AA-mediated cardioprotection and energy metabolism. Neonatal cardiomyocytes were treated with DMSO, shAMPK-NC, shAMPK, LY204002 (LY; 20 μ mol/L), GSK690693 (GSK; 10 μ mol/L) and/or AA (10 μ mol/L), then subjected to OGD insult. **a** LDH release analysis in isolated cardiomyocytes. **b** Cell viability in cardiomyocytes was also analyzed. **c** TUNEL assay was performed and analyzed in mouse cardiomyocytes. Bar: 50 μ m. **d**, **e** ATP level (**d**) was determined and PCr/ATP ratio was calculated (**e**). $n = 6$ independent experiments. * $P < 0.05$, ** $P < 0.01$ vs. OGD + AA 10 + shAMPK-NC. # $P < 0.05$ vs indicated group, N.S. indicates no significance. Data are presented as the mean \pm SEM.

injury, indicating that both glycophagy and mitophagy are critical for the cardioprotective roles of AA. Therefore, AA may be a multifunctional cardioprotective regulator that increases glycogen utilization by promoting glycophagy and glycolysis and also enhances cardiomyocyte resistance to ischemia, and reduces excessive energy consumption by promoting mitophagy. The PI3K/Akt and AMPK pathways have overlapping effects on

myocardial protection [48, 49]; thus, the upstream pathways of the two after AA treatment are worth further investigation.

In conclusion, our results demonstrated that AA improved recovery from myocyte injury, myocardial dysfunction, and energy metabolism disorders after MI by regulating mitophagy to maintain mitochondrial homeostasis and by modulating glycophagy and glycolysis to increase glycogen utilization.

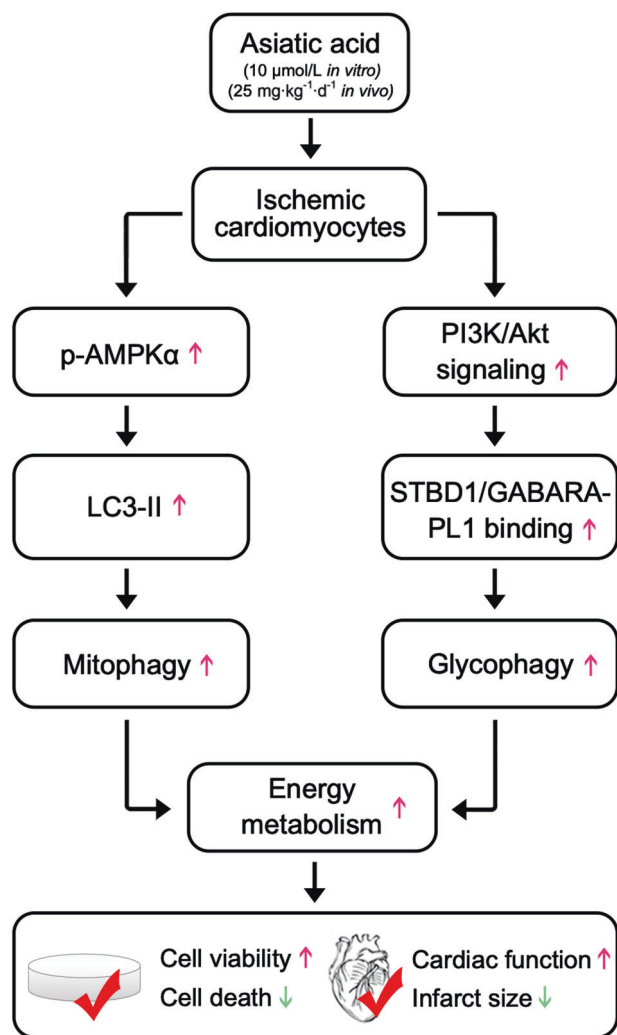


Fig. 8 A proposed model for the cardioprotection of AA in MI heart and OGD cardiomyocytes. AA modulates mitophagic and glycopyhagic level in isolated OGD cardiomyocytes and/or MI mice myocardium through the activation of the AMPK α and PI3K/Akt signaling pathways, thereby contributing to the increased energy metabolism and cardioprotection of AA in vivo and in vitro. Red arrows indicate the promotion, and green arrows indicate the reduction.

ACKNOWLEDGEMENTS

This work was supported by the National Key Research and Development Program of China (2017YFA0105600, 2020YFA0112600), the National Natural Sciences Foundation of China (81870208, 82070260), the Shanghai Pujiang Program (19PJ1408900), the Shanghai Animal Research Program (211440901800), the Science and Technology Development Fund of Shanghai Pudong New Area (PKJ2020-Y23), Shanghai Engineering Research Center of Artificial Heart and Heart Failure Medicine (19DZ2251000), the Major Program of Development Fund for Shanghai Zhangjiang National Innovation Demonstration Zone < Stem Cell Strategic Biobank and Stem Cell Clinical Technology Transformation Platform > (ZJ2018-ZD-004), and the Peak Disciplines (Type IV) of Institutions of Higher Learning in Shanghai.

AUTHOR CONTRIBUTIONS

FQ analyzed the data, designed the study, and wrote the manuscript. FQ, YY, WL, and YSG performed the experiments. ZMZ, ZML, and LG provided technical support and substantial contributions to the conception and design of the study. ZML and LG directed the study, managed the project, interpreted the data, and co-wrote the manuscript.

ADDITIONAL INFORMATION

Supplementary information The online version contains supplementary material available at <https://doi.org/10.1038/s41401-021-00763-9>.

Competing interests: The authors declare no competing interests.

REFERENCES

1. Yeh RW, Sidney S, Chandra M, Sorel M, Selby JV, Go AS. Population trends in the incidence and outcomes of acute myocardial infarction. *N Engl J Med*. 2010;362:2155–65.
2. Roger VL, Go AS, Lloyd-Jones DM, Adams RJ, Berry JD, Brown TM, et al. Heart disease and stroke statistics—2011 update: a report from the American Heart Association. *Circulation*. 2011;123:e18–e209.
3. Saito T, Sadoshima J. Molecular mechanisms of mitochondrial autophagy/mitophagy in the heart. *Circ Res*. 2015;116:1477–90.
4. Lorentzon M, Ramunddal T, Bollano E, Soussi B, Waagstein F, Omerovic E. In vivo effects of myocardial creatine depletion on left ventricular function, morphology, and energy metabolism—consequences in acute myocardial infarction. *J Card Fail*. 2007;13:230–7.
5. Schaneberg BT, Mikell JR, Bedir E, Khan IA. An improved HPLC method for quantitative determination of six triterpenes in *Centella asiatica* extracts and commercial products. *Pharmazie*. 2003;58:381–4.
6. Tsao SM, Yin MC. Antioxidative and antiinflammatory activities of asiatic acid, glycyrrhizic acid, and oleanolic acid in human bronchial epithelial cells. *J Agric Food Chem*. 2015;63:3196–204.
7. Lu Y, Kan H, Wang Y, Wang D, Wang X, Gao J, et al. Asiatic acid ameliorates hepatic ischemia/reperfusion injury in rats via mitochondria-targeted protective mechanism. *Toxicol Appl Pharmacol*. 2018;338:214–23.
8. Chao PC, Yin MC, Mong MC. Anti-apoptotic and anti-glycative effects of asiatic acid in the brain of *D-galactose* treated mice. *Food Funct*. 2015;6:542–8.
9. Maquart FX, Chastang F, Simeon A, Birembaut P, Gillery P, Wegrowski Y. Triterpenes from *Centella asiatica* stimulate extracellular matrix accumulation in rat experimental wounds. *Eur J Dermatol*. 1999;9:289–96.
10. Grimaldi R, De Ponti F, D'Angelo L, Caravaggi M, Guidi G, Lecchini S, et al. Pharmacokinetics of the total triterpenic fraction of *Centella asiatica* after single and multiple administrations to healthy volunteers. A new assay for asiatic acid. *J Ethnopharmacol*. 1990;28:235–41.
11. Lee KY, Bae ON, Serfozo K, Hejebian S, Moussa A, Reeves M, et al. Asiatic acid attenuates infarct volume, mitochondrial dysfunction, and matrix metalloproteinase-9 induction after focal cerebral ischemia. *Stroke*. 2012;43:1632–8.
12. Kubli DA, Gustafsson AB. Mitochondria and mitophagy: the yin and yang of cell death control. *Circ Res*. 2012;111:1208–21.
13. Kim J, Kundu M, Viollet B, Guan KL. AMPK and mTOR regulate autophagy through direct phosphorylation of Ulk1. *Nat Cell Biol*. 2011;13:132–41.
14. Hardie DG. AMPK: a key regulator of energy balance in the single cell and the whole organism. *Int J Obes (Lond)*. 2008;32:57–12. Suppl 4.
15. Fritzen AM, Fosrig C, Jeppesen J, Jensen TE, Lundsgaard AM, Serup AK, et al. Role of AMPK in regulation of LC3 lipidation as a marker of autophagy in skeletal muscle. *Cell Signal*. 2016;28:663–74.
16. Zhao H, Tang M, Liu M, Chen L. Glycopyhagy: an emerging target in pathology. *Clin Chim Acta*. 2018;484:298–303.
17. Kotoulas OB, Kalamidas SA, Kondomerkos DJ. Glycopyhagy in glucose homeostasis. *Pathol Res Pr*. 2006;202:631–8.
18. Delbridge LM, Mellor KM, Taylor DJ, Gottlieb RA. Myocardial autophagic energy stress responses—macroautophagy, mitophagy, and glycopyhagy. *Am J Physiol Heart Circ Physiol*. 2015;308:H1194–204.
19. Jiang S, Heller B, Tagliabracci VS, Zhai L, Irimia JM, DePaoli-Roach AA, et al. Starch binding domain-containing protein 1/genethonin 1 is a novel participant in glycogen metabolism. *J Biol Chem*. 2010;285:34960–71.
20. Jiang S, Wells CD, Roach PJ. Starch-binding domain-containing protein 1 (Stbd1) and glycogen metabolism: Identification of the Atg8 family interacting motif (AIM) in Stbd1 required for interaction with GABARAPL1. *Biochem Biophys Res Commun*. 2011;413:420–5.
21. Sun M, Ouzounian M, de Couto G, Chen M, Yan R, Fukuoka M, et al. Cathepsin-L ameliorates cardiac hypertrophy through activation of the autophagy-lysosomal dependent protein processing pathways. *J Am Heart Assoc*. 2013;2:e000191.
22. Yuan Y, Zheng Y, Zhang X, Chen Y, Wu X, Wu J, et al. BNIP3L/NIX-mediated mitophagy protects against ischemic brain injury independent of PARK2. *Autophagy*. 2017;13:1754–66.
23. Yang H, Shen H, Li J, Guo LW. SIGMAR1/Sigma-1 receptor ablation impairs autophagosome clearance. *Autophagy*. 2019;15:1539–57.

24. Reichert K, Colantuono B, McCormack I, Rodrigues F, Pavlov V, Abid MR. Murine left anterior descending (LAD) coronary artery ligation: an improved and simplified model for myocardial infarction. *J Vis Exp*. 2017;122:55353.
25. Hardy CJ, Weiss RG, Bottomley PA, Gerstenblith G. Altered myocardial high-energy phosphate metabolites in patients with dilated cardiomyopathy. *Am Heart J*. 1991;122:795–801.
26. Herzig S, Shaw RJ. AMPK: guardian of metabolism and mitochondrial homeostasis. *Nat Rev Mol Cell Biol*. 2018;19:121–35.
27. Mellor KM, Varma U, Stapleton DI, Delbridge LM. Cardiomyocyte glycophyagy is regulated by insulin and exposure to high extracellular glucose. *Am J Physiol Heart Circ Physiol*. 2014;306:H1240–5.
28. Marchand B, Arsenault D, Raymond-Fleury A, Boisvert FM, Boucher MJ. Glycogen synthase kinase-3 (GSK3) inhibition induces pro-survival autophagic signals in human pancreatic cancer cells. *J Biol Chem*. 2015;290:5592–605.
29. Reichelt ME, Mellor KM, Curl CL, Stapleton D, Delbridge LM. Myocardial glycophyagy - a specific glycogen handling response to metabolic stress is accentuated in the female heart. *J Mol Cell Cardiol*. 2013;65:67–75.
30. Cheng W, Wu P, Du Y, Wang Y, Zhou N, Ge Y, et al. Puerarin improves cardiac function through regulation of energy metabolism in streptozotocin-nicotinamide induced diabetic mice after myocardial infarction. *Biochem Biophys Res Commun*. 2015;463:1108–14.
31. Lim SH, Lee J. Xyloglucan intake attenuates myocardial injury by inhibiting apoptosis and improving energy metabolism in a rat model of myocardial infarction. *Nutr Res*. 2017;45:19–29.
32. Qiu F, Zhang H, Yuan Y, Liu Z, Huang B, Miao H, et al. A decrease of ATP production steered by PEF in cardiomyocytes with oxygen-glucose deprivation is associated with an AMPK-dependent degradation pathway. *Int J Cardiol*. 2018;257:262–71.
33. Huo L, Shi W, Chong L, Wang J, Zhang K, Li Y. Asiatic acid inhibits left ventricular remodeling and improves cardiac function in a rat model of myocardial infarction. *Exp Ther Med*. 2016;11:57–64.
34. Dai Y, Wang Z, Quan M, Lv Y, Li Y, Xin HB, et al. Asiatic acid protects against myocardial ischemia/reperfusion injury via modulation of glycometabolism in rat cardiomyocyte. *Drug Des Devel Ther*. 2018;12:3573–82.
35. Moloudizargari M, Asghari MH, Ghobadi E, Fallah M, Rasouli S, Abdollahi M. Autophagy, its mechanisms and regulation: Implications in neurodegenerative diseases. *Ageing Res Rev*. 2017;40:64–74.
36. Komatsu M, Ichimura Y. Selective autophagy regulates various cellular functions. *Genes Cells*. 2010;15:923–33.
37. Johansen T, Lamark T. Selective autophagy mediated by autophagic adapter proteins. *Autophagy*. 2011;7:279–96.
38. Matsui Y, Takagi H, Qu X, Abdellatif M, Sakoda H, Asano T, et al. Distinct roles of autophagy in the heart during ischemia and reperfusion: roles of AMP-activated protein kinase and Beclin 1 in mediating autophagy. *Circ Res*. 2007;100:914–22.
39. Sciarretta S, Zhai P, Shao D, Maejima Y, Robbins J, Volpe M, et al. Rheb is a critical regulator of autophagy during myocardial ischemia: pathophysiological implications in obesity and metabolic syndrome. *Circulation*. 2012;125:1134–46.
40. Buss SJ, Muenz S, Riffel JH, Malekar P, Hagenmueller M, Weiss CS, et al. Beneficial effects of mammalian target of rapamycin inhibition on left ventricular remodeling after myocardial infarction. *J Am Coll Cardiol*. 2009;54:2435–46.
41. Egan DF, Shackelford DB, Mihaylova MM, Gelino S, Kohnz RA, Mair W, et al. Phosphorylation of ULK1 (hATG1) by AMP-activated protein kinase connects energy sensing to mitophagy. *Science*. 2011;331:456–61.
42. Sinha RA, Singh BK, Zhou J, Wu Y, Farah BL, Ohba K, et al. Thyroid hormone induction of mitochondrial activity is coupled to mitophagy via ROS-AMPK-ULK1 signaling. *Autophagy*. 2015;11:1341–57.
43. Itakura E, Kishi-Itakura C, Koyama-Honda I, Mizushima N. Structures containing Atg9A and the ULK1 complex independently target depolarized mitochondria at initial stages of Parkin-mediated mitophagy. *J Cell Sci*. 2012;125:1488–99.
44. Lazarou M, Sliter DA, Kane LA, Sarraf SA, Wang C, Burman JL, et al. The ubiquitin kinase PINK1 recruits autophagy receptors to induce mitophagy. *Nature*. 2015;524:309–14.
45. Zhu J, Wang KZ, Chu CT. After the banquet: mitochondrial biogenesis, mitophagy, and cell survival. *Autophagy*. 2013;9:1663–76.
46. Hanna RA, Quinsay MN, Orogo AM, Giang K, Rikka S, Gustafsson AB. Microtubule-associated protein 1 light chain 3 (LC3) interacts with Bnip3 protein to selectively remove endoplasmic reticulum and mitochondria via autophagy. *J Biol Chem*. 2012;287:19094–104.
47. Nielsen J, Ortenblad N. Physiological aspects of the subcellular localization of glycogen in skeletal muscle. *Appl Physiol Nutr Metab*. 2013;38:91–9.
48. Chen K, Li G, Geng F, Zhang Z, Li J, Yang M, et al. Berberine reduces ischemia/reperfusion-induced myocardial apoptosis via activating AMPK and PI3K-Akt signaling in diabetic rats. *Apoptosis*. 2014;19:946–57.
49. Sun Y, Jiang C, Jiang J, Qiu L. Dexmedetomidine protects mice against myocardium ischaemic/reperfusion injury by activating an AMPK/PI3K/Akt/eNOS pathway. *Clin Exp Pharmacol Physiol*. 2017;44:946–53.